Physicochem. Probl. Miner. Process., 56(1), 2020, 54-64

http://www.journalssystem.com/ppmp

Physicochemical Problems of Mineral Processing

ISSN 1643-1049

Received July 11, 2019; reviewed; accepted October 11, 2019

Use of bubble load to interpret particle transport across the pulp-froth interface in a flotation cell

Clayton Bhondayi

Institute for the Development of Energy for African Sustainability, University of South Africa, Florida, South Africa

Corresponding author: cbhondayi@gmail.com

Abstract: This work demonstrates the use of bubble loads to understand the transport of particles across the pulp-froth interface in a flotation cell processing an Upper Group 2 chromitite seam (UG2) ore. Bubble loads were measured on the first primary cleaner cell of an operating flotation plant using a bubble load meter with a 20mm riser diameter. A bubble load value of 10.58grams/liter was obtained. The bubble load data was used to understand, entrainment and dropback of chromite as a function of particle size. By defining terms such as froth flow number and net dropback, it was found that chromite (known to be non-floatable) was also recovered through true flotation. The entrainment of chromite was found to be predominantly in -25 μm size while +25 μm size particles were found to be floatable and highly susceptible to dropping back. Net-dropback of chromite particles was found to increase with a decrease in chromite particle size contrary to expectation. An overall froth flow number of 69% was obtained.

Keywords: bubble loading, entrainment, true flotation, froth flow number, dropback

1. Introduction

Transport of particles between the pulp-phase and the froth phase can take place through the following routes (1) by collision with and attachment to a bubble conventionally called true flotation (2) hydraulic entrainment of particles by water (3) entrapment of unattached particles between attached particles and, (4) particles dropping back from the froth. The sum of these transport mechanisms determines the type and quantity of particles that eventually report to the concentrate. True flotation and entrainment transport particles to the froth and are functions of pulp phase conditions. Froth dropback transport particles from the froth to the pulp and it depends on the froth phase sub-processes. While particle entrainment and entrapment are non-selective based on the physicochemical conditions of particles, 'true' flotation is selective and underpins the success of the flotation process. Froth drop back can either be selective or non-selective. Moys (1979) defined a selective froth as one in which particles reattach to the available space in the froth based on some property e.g. particle hydrophobicity or particle size.

True flotation can be measured using the concept of bubble loading. Bubble load represents the apparent density of a bubble-particle aggregate (g/L) entering the froth (Yianatos et al., 2008). It is governed by pulp-phase sub-processes which include bubble particle collision, attachment, and possible detachment. The importance of bubble load as a criterion for evaluating flotation kinetics has long been recognized. King et al. (1974), performed single bubble experiments showing how bubble-load increases as the bubble rise through the pulp phase. Subsequently, several methods (Dyer, 1995; Seaman et al. 2004; Moys, 2010; Bhondayi and Moys, 2011) to measure bubble loading in industrial flotation cells were developed. Although these methods or their variants are used extensively, they have limitations. Moys et al. (2010) state that bubble load values taken just below the pulp-froth interface do not account for any additional attachment or detachment that may take place as the bubble hits the interface. Bhondayi and Moys (2011) provide a summary of some of the limitations associated with bubble load measuring methods. The limitations include particle losses in the riser, entrainment of

DOI: 10.5277/ppmp19077

unattached particles into the riser, displacement of heavily laden bubbles at the riser entrance. They, however, concluded that some of the limitations can be eliminated by designing the riser diameter correctly. They recommended a riser diameter of 20mm. Work on bubble loading and how it can be used to understand the flotation process is taking place despite the limitations e.g. Seaman et al. (2004) developed a device to measure bubble loading and used the bubble load result to estimate froth recovery and froth selectivity. Yianatos et al. (2008) developed equation [1] to estimate froth recovery (R_f) using bubble load information. Recently, Chengeni et al. (2016) and Eskanlou et al. (2017) used a bubble load meter similar in concept to that developed by Bhondayi and Moys (2011) to assess variation of bubble loads as a function of height in column flotation.

$$R_f = \frac{C.X_C - R_{Ef}.E.X_E}{\lambda_B.J_G.A_C.X_B} \quad (1)$$

where C (tph) as the overall concentrate mass flowrate; X_C is the mineral (or valuable species) grade in the concentrate;λ_B the bubble load (kg/m^3); $X_B$is bubble load grade;J_G superficial gas velocity (m/s) and A_C (m^2) cell cross-sectional area at the interface level; E (tph) is the mass transport by entrainment across the pulp froth interface; X_E is the grade of entrained mineral recovered by entrainment and R_{EF} is the froth recovery of entrained particles.

Equation (1) indicates that froth recovery is a measure of the cumulative effect of all particle transport mechanisms across the pulp froth interface. It also shows that to evaluate froth recovery using bubble loads, either the non- selective entrainment of particle or dropback of particles from the froth must be known. In this work, the bulk transport of particles across the pulp-froth interface is inferred from bubble load and concentrate flowrates. Two new parameters (1) froth flow number and (2) net-drop back are defined using bubble load and total concentrate flow rates only. These parameters are used to assess the relative movement of particles across the pulp-froth interface as a function of particle size. General heuristics to assess flotation performance based on these parameters is provided.

2. Materials and methods

2.1. UG2 ore composition and mineralogy

Experiments in this work were carried out at Lonmin's Eastern Platinum Concentrator (EPC) which processes UG2 ore obtained from Western Limp of the Bushveld Complex in South Africa. The Bushveld Complex contains the largest concentration of Platinum Group Elements (PGEs) in the world (Cawthorn, 2005; Cawthorn, 2010). The PGEs are concentrated in three mineralized zones viz. Merensky Reef, Upper Group Two Reef (UG2) and the Platreef.According to Vermark (1995), the major mineral phases of the UG2 ore are chromite (60 -90%w/w), orthopyroxene (5- 30% w/w) and, plagioclase (1-10% w/w) while the minor mineral phases include; phlogopite, biotite, clinopyroxene, ilmenite, rutile, magnetite and, base metal sulphides (mainly chalcopyrite, pyrrhotite, pyrite and, pentlandite). The PGEs are associated with base metal sulfides, silicate and or chromite grains (McLaren and De Villiers, 1982; Hay and Roy, 2010) and typically occur as assemblages of Platinum Group Minerals (PGMs). The main PGMs include sulfides (laurite (RuS_2), cooperate (PeS), malanite (Pt-Ir-Rh-Cu sulfide) and, braggite ([Pt, Pd, Ni]S)), platinum alloys with Iron (Pt-Fe), platinum tellurides and, platinum arsenides (McLaren and De Villiers, 1982). The specific mineral composition of the ore used in this work is summarised in Table 1.

2.2. Flotation circuit

Bubble load measurements were done on the first cell of the primary cleaners for a platinum concentrator processing UG2 Ore (Fig. 1). The ore is typically ground to 80% passing 75µm and treated with Sodium N-Propyl Xanthate (SNPX) collector dosed at a rate of 150g/t with Dowfroth and Carboxymethyl Cellulose (CMC) as frother and depressant respectively. Copper sulfate is also added as an activator. The conditioned slurry is typically pumped from the primary rougher feed tank at a rate of 415tph at 22% w/w solids into the first cell of the primary roughers. Concentrate from the first three cells of the primary roughers goes to the first three cells of the primary cleaners, while the rest goes to the last 6 cells of the primary cleaners. Concentrate from these first three cleaner cells is pumped to the high-high grade 'HHG' concentrate cells as shown in the basic flow diagram, Fig. 1. This process

typically concentrates PGMs in the ore from 4g/t to 100g/t (Harris, 2000) and the smelter expects chromite typically quantified as percentage chromium oxide (%Cr_2O_3) concentration below 3% (Hay and Roy, 2010). Concentrate with chromium oxide above 3% incurs a penalty from Smelters because it increases the build-up of chromite spinel inside the smelter reducing its operational volume (Philip et al., 2008; Hay and Roy, 2010).

Table 1. Typical UG 2 composition (Bhondayi, 2010)

Mineral		%Composition	Density(kg/m^3)
Pyroxene	Clinopyroxene ($CaAl_2SiO_6$) Orthopyroxene ($MgSiO_3$)	38.4	3200-3380
Chromite	$FeCr_2O_4$	36.8	4320-4570
Feldspar	Anorthite Albite Potash Spar	17.5	2560-2760
Olivine	Mg_2SiO_4, Ca_2SiO_4, Mn_2SiO_4 $FeSiO_4$, Co_2SiO_4, $NiSiO_4$	0.6	3300
Alteration silicates		3.9	
Other Silicates		1.7	
Base Metal Sulphides		0.3	
Other		0.8	
Total		**100**	

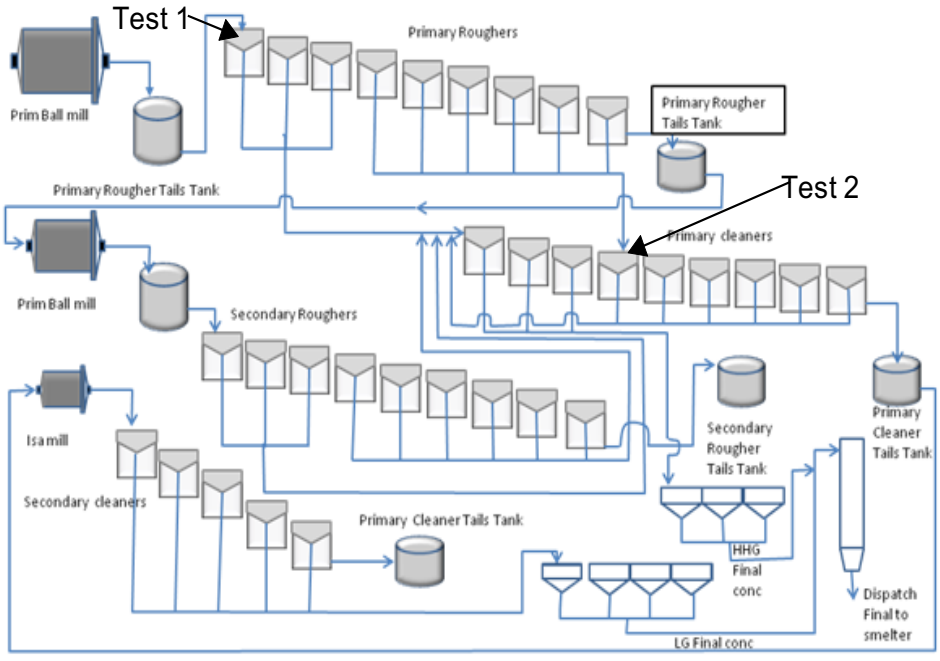

Fig. 1. Flow diagram PGM concentrator showing the position of bubble load measurement (test 2) (Bhondayi, 2010)

2.3. Bubble load measurement procedure

The bubble load meter designed by Bhondayi and Moys, (2011) was used to measure bubble loading. Briefly, this consists of two sections viz. the collection chamber and the riser. The procedure to measure

bubble loading in an industrial setting was as follows: (1) The collection chamber was filled with frother/plant water, (2) The pump was started after making sure that the bottom of the riser section of the device was tightly closed (3) circulation was allowed to take place until all the sections of the device were filled with water (4) The device was lowered into the flotation cell, down to the required level and while the pump was still circulating water, the stopper at the bottom of the device was removed, (6) The timing device was started as the first bubbles entered the collection chamber (7) After running for required time, the valve to the collection chamber was closed and time and volume recorded. The water in the collection chamber was filtered and combined with mass captured by the filter to constitute the mass of the sample collected per run. Fig. 2 is a schematic of the bubble load measurement process.

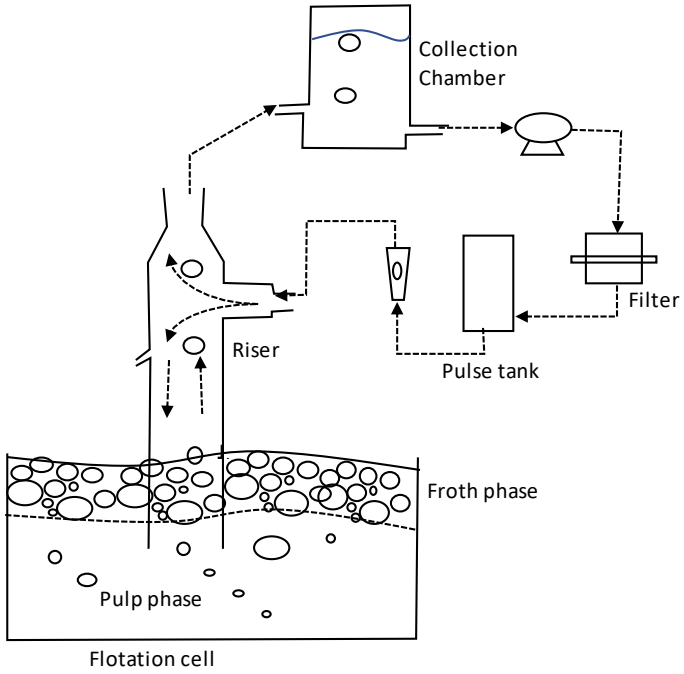

Fig. 2. Illustration of the bubble load measuring methodology

2.4. Concentrate and pulp sampling procedure

The sampling of concentrate from the cell where bubble load was measured was done manually using buckets, A3 plastic bags, and a timer. The concentrate samples were obtained by cutting the whole stream of concentrate from concentrate launder while timing the duration of the cut. Samples of the pulp were drawn just below the pulp-froth interface using a beaker. The beaker was dipped to below the pulp froth interface while closed but facing upwards opening was done in the pulp phase. This was done to make sure that only the pulp is sampled without sampling particles that are attached to bubbles.

3. Results and discussion

3.1. Bubble load rate and froth flow number

The measurement of bubble load was done continuously for about 10 minutes with strict monitoring of pressure drop across the filter, a bubble load of 10.45g/liter of air was obtained as summarised in Table 2. Preliminary experiments on a rougher flotation cell had established a relative standard deviation of 15.74% in bubble load values (Bhondayi, 2010). It is also important to note that, while Seaman et al. (2004) measured bubble loads for a duration of 2mins and proved repeatability of the procedure, results in Table 2 were obtained in 5 times the duration used by Seaman *op cit*. and thus it can be assumed that any variations in bubble load were smoothened out by the longer duration. The bubble load value obtained in this work is lower than the bubble load values that were obtained by Seaman et al. (2004) (Zinc concentrator) and Yianatos et al. (2010) (Copper concentrator). This was attributed to the difficulty in floating PGMs especially the UG2 ore.The froth flow number (R_{fn}) herein is defined as the ratio of concentrate mass flowrate to bubble load mass flowrate was found to be circa 69% indicating net particle

dropback in the froth. Note that, froth flow number is different from the froth recovery (R_f) because it does not distinguish particles recovered by entrainment and those recovered by true flotation, thus it can take any number above zero while the froth recovery (R_f) can only assume a value between 0 and 1. When the contribution of entrainment is negligible, the froth flow number becomes the froth recovery.

The froth flow number can be used to gauge the performance of the froth if the bubble load meter is known to work correctly.When$R_{fn} > 1$,this points to high entrainment recovery to the froth while a froth flow number$0 < R_{fn} < 1$, indicates that there is particle dropback in the froth with a number close to zero indicating high particle dropback.

Table 2. Bubble load results

Time (sec)	Air volume (cm^3)	Jg (cm/s)	Mass (g)	Bubble load (g/l)	Concentrate loading (g/l)	Froth flow number
592	3404	0.81	35.58	10.45	2.46	0.69

3.2. Analysis of grade in the bubble load, concentrate, and pulp

To reduce costs associated with Platinum Group Elements (PGEs) analysis, it was decided to analyze for base metal sulfides (nickel and copper) and chromite as the basis for understanding particle transport across the interface. Fig. 3 to Fig. 6 shows the variation of floatable elements including chromite as a function of particle size in bubble load, concentrate, and pulp samples. Note that error bars are not included in the work as costs of sample analysis and sample availability precluded repeats. More importantly, this work is focused on demonstrating use of bubble load data to infer particle transport across the interface.

Figs. 3, 4 and 5 show that the percentage of sulfides/floatable component increases with the particle sizes in each of the three respective samples; the bubble load has the highest sulfide content per size class while the pulp has the lowest. Interestingly, the grade of concentrate follows the bubble load. This points to the upgrading nature of the flotation process since bubble loading is the main path by which particles are transported to the froth. Furthermore, this can also be interpreted as indicating entrainment (dilution of bubble loads in concentrate) may not be significant because the grade of concentrate and bubble load are almost similar. Fig. 6 shows the variation of $\%Cr_2O_3$ with particle size in the bubble load, pulp and concentrate. The figure indicates that for -25 μm range, the pulp has the highest concentration of chromite while bubble load has the lowest concentration. A difference of circa 1.7% w/w in Cr_2O_3 concentration is observed between bubble load and concentrate grade indicating entrainment in this size class. For coarser size classes, the trends change. It is interesting to note the presence of significant amounts of Cr_2O_3 in the bubble load (3.83% in +106 μm and 3.80% in (-75+53 μm) indicating that chromite was also reporting to the concentrate not only by entrainment but maybe also attached to bubbles. The chromite in the bubble load may be a result of entrapment between attached particles or chromite floated as composites encased by fully liberated floatable components. It may also be possible that the chromite was activated in the pulp and therefore floated. However, this is least likely as chromite is generally considered naturally hydrophilic. It is known to be activated when it adsorbs copper in the form of Cu (OH) + at pH 9 (Wesseldijk et al., 1999). Copper sulfate has been identified as one reagent that results in chromite activation when it is used as an activator in PGM flotation (Ekmekci et al., 2003). Thus, the presence of chromite in the bubble load and the possibility of it being recovered through true flotation imply that chromite can no longer be considered as a completely non-floatable gangue in the estimation of entrainment.

3.3. Estimation of entrainment

Calculation of the degree of entrainment requires that tracer experiments with a non-floatable component with sizes classes that matches the feed be done. In this work, tracer experiments were not performed and therefore bubble load data and the abundant chromite in the feed were used to estimate entrainment. The total mass of chromite in the feed and in each size class was calculated using mass balance after assuming that the concentration of particles in each size class in the pulp is similar to that

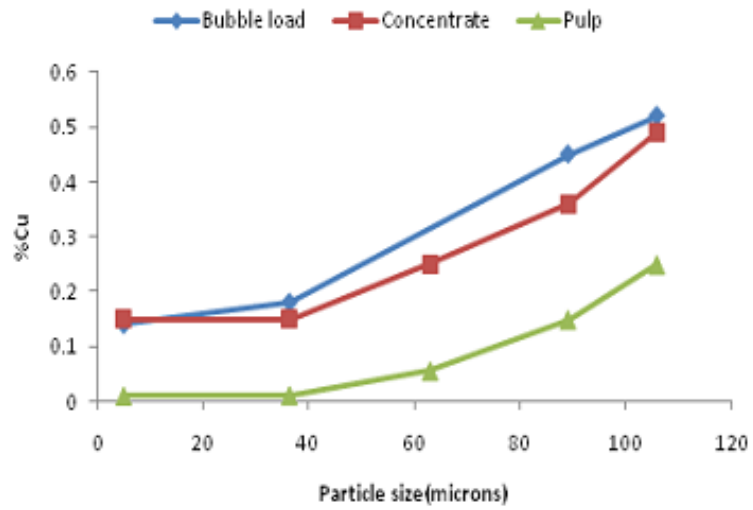

Fig. 3. Variation of %Cu with particle size in bubble load, concentrate, and pulp samples

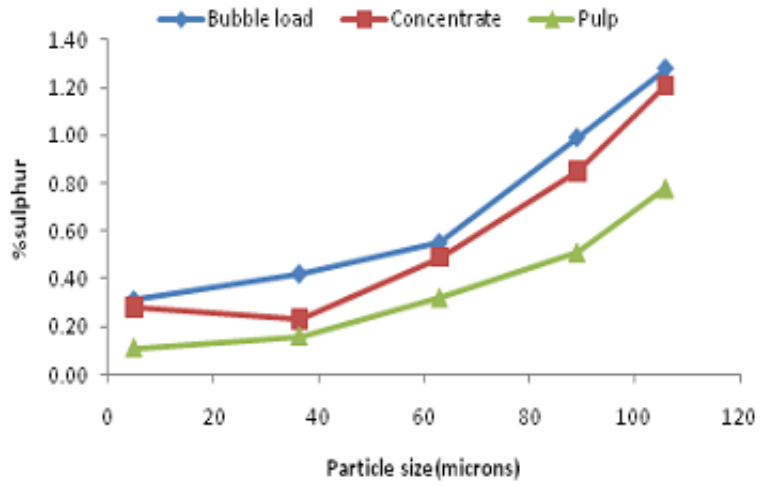

Fig. 4. Variation of %Sulphide with particle size in bubble load, concentrate, and pulp samples

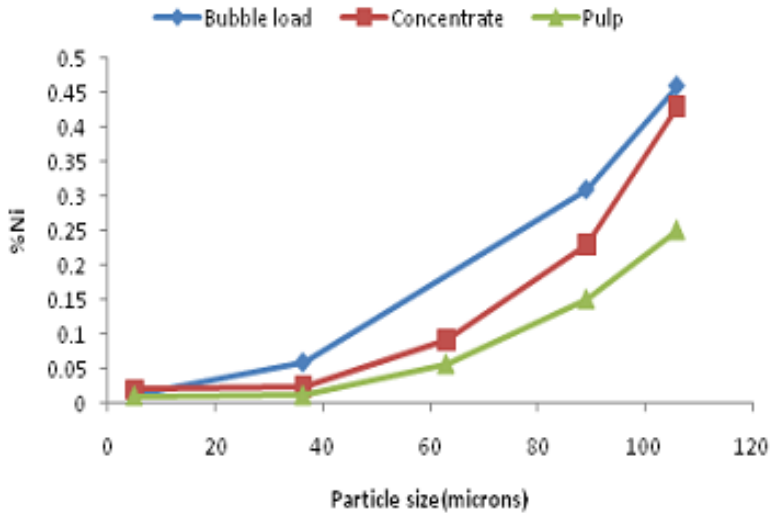

Fig. 5. Variation of %Ni with particle size in bubble load, concentrate, and pulp samples

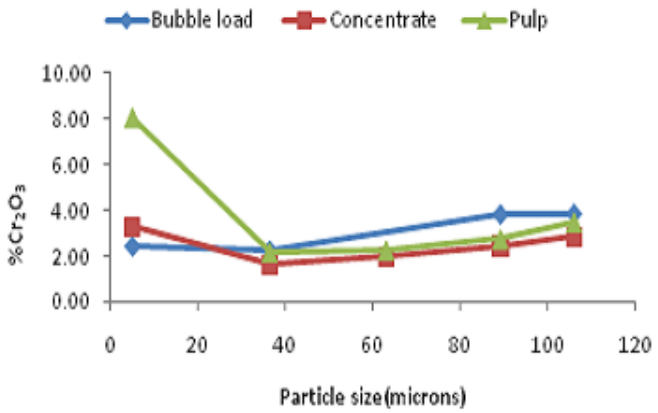

Fig. 6. Variation of $\%Cr_2O_3$ with particle size in bubble load, concentrate, and pulp samples

in the tailings. The rate at which particles are transferred from the pulp phase to the froth phase by true flotation (B) was calculated from the bubble load and superficial gas velocity and the cross-sectional area of the flotation cell i.e. $B = \lambda_B . J_G . A_C$ as given by Yianatos et al. (2008). Inherent in these calculations the assumption that superficial gas velocity (J_G) and the bubble load (λ_B) was uniform across the flotation cell. Table 3 shows the mass flowrate in each size class and chromite content in each size class in the feed, concentrate and bubble load streams. Fig. 7 summarises the flowrates in bubble load and concentrate streams. The data (Table 3) indicates that 3.34% (41.35 g/s) of the total chromite in the feed is reporting to the concentrate, 5.34% (66.03 g/s) is attaching to bubbles and 91.32% (1237.25 g/s) of the original chromite in the feed is reporting to the tailings. Cumulatively, 2.42% of the total concentrate flow is chromite. This is within the acceptable range of chromite required at the smelter. Fig. 7 also shows interesting trends, where fines (-25 µm) constitute the largest portion of chromite in the concentrate while the bubble load curve exhibits the classical bell-shaped curve of recovery as a function of particle sizes. In this case, the -53+25µm range was highly floatable compared to other sizes. The relative position of the two curves indicates dropback of particles except for the -25µm size which shows that chromite was added to the concentrate by a route other than attachment to bubbles.

Table 3: Mass flow rate of chromite per size class in each stream

Size class	Mass flow rate Cr_2O_3 in Size class (g/s) in Feed	Mass flow rate Cr_2O_3 in Size class (g/s) in concentrate	Mass flow rate Cr_2O_3 in Size class (g/s) by True flotation
(-150+106)	55.47	6.53	9.55
(-106+75)	67.11	8.06	12.53
(-53+25)	189.49	10.61	31.99
-25	925.18	16.15	11.95
Total	**1237.25**	**41.35**	**66.02**

3.4. Estimation of net-froth dropback

Froth dropback (B') for true flotation is normally defined as the mass flowrate of the chromite that was collected by true flotation/ bubble load flowrate (B) that does not report to the concentrate. Similarly, the dropback for entrained particles (E') represents the mass flowrate of previously entrained particles that drops back to the pulp (see Fig. 8). It can also be shown that the total dropback (D_T) is given by equation (5).

$$D_T - E = B - C_T \tag{5}$$

This definition requires a measure of entrainment contribution (E) to the concentrate flow. In the absence of such a measure or its estimate, equation (5) can be used to assess relative movement of

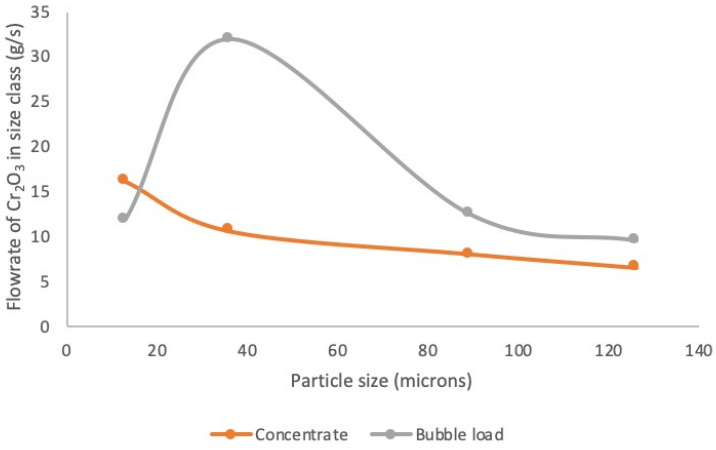

Fig. 7. Mass flow rate of chromite per size class in bubble load and concentrate streams

particles. Net-dropback is defined as the difference between bubble load flowrate per size class and the mass flowrate per size class in concentrate (C_T), i.e. ($B - C_T$). This can be used to assess whether there is a net drop or entrainment into the froth per given size class. Consider three cases:

1) Case 1: $(B - C_T) < 0$;

If the mass flowrate of chromite in the concentrate is higher than the mass flowrate of chromite in the bubble load per size class (negative net-dropback), it means particles were entrained into the froth and therefore entrainment is dominant.

2) Case 2:$(B - C_T) > 0$;

When net dropback is positive, this implies particles dropping back from the froth and the contribution by entrainment could be small.

3) Case 3: $(B - C_T) = 0$.

This implies net dropback is equivalent to total entrainment, and for particle size range less susceptible to entrainment it means that particles collected by bubbles will be recovered to the concentrate. Fig. 9, shows that the percentage of drop back increases with a decrease in particle size i.e. from 31.60% for the (-150 +106) µm up to 66.83% for (-53+25) µm. This increase can be explained by acknowledging that the degree of 'locking' of the chromite would decrease with particle size, meaning that smaller particles have a higher degree of Cr_2O_3 liberation. Minerals with a high grade of Cr_2O_3 can only be floated when they are partially activated, thus they are weakly floatable. These particles are highly likely to be rejected preferentially in the froth phase. This phenomenon seems to counteract

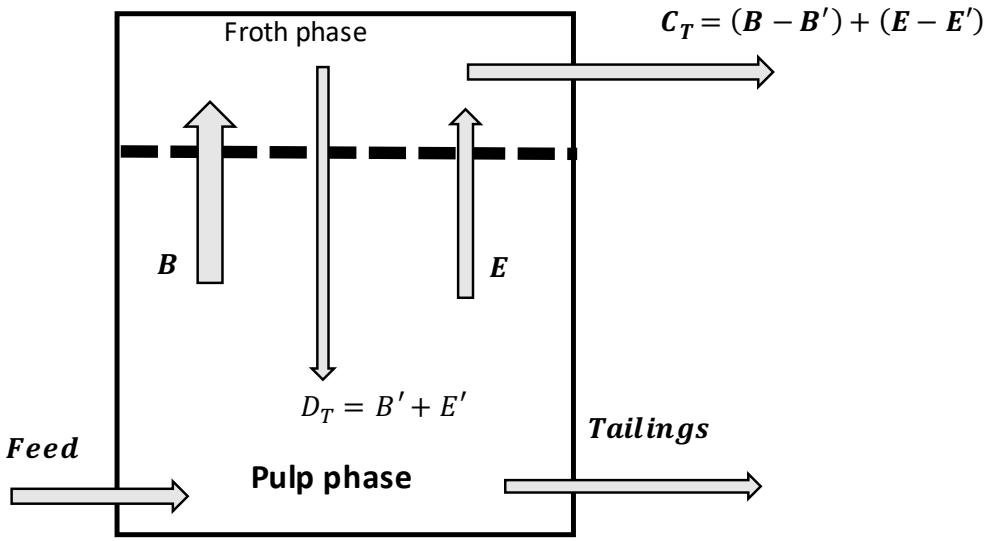

Fig. 8. Illustration of the flow of chromite particles across the pulp-froth interface

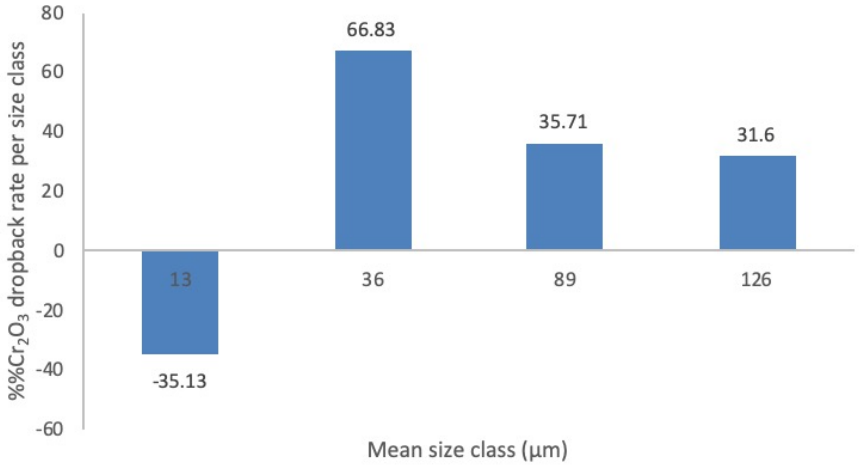

Fig. 9. Comparison of the chromite content of bubble load and concentrate

the effect of particle settling velocity, finer particles have inferior settling velocities than coarser particles of the same mineral, thus it was expected that the drop back would increase with particle sizes. This observation may mean that the froth phase is selective towards the more hydrophobic particles, in this case, the floatable mineral with a low degree of liberation of chromite particles. The negative value for -25 µm size class indicates that entrainment is also adding particles of chromite to the froth phase and hence the concentrate. This extra 35.13% of the -25 µm indicates excessive entrainment. This observation is in tandem with the generally accepted view that entrainment or degree of entrainment increases with a decrease in particle sizes i.e. (Savassi et al., 1998; Zheng et al., 2006).

Conclusions

The bubble load meter reported by Bhondayi and Moys (2011) was used to measure bubble load in an industrial flotation cell processing UG2 ore. A bubble load value of 10.58grams/liter was obtained.This value was found to be low when compared to results obtained in a Zinc concentrator (Seaman et al. 2004) and Copper concentrator (Yianotos et al. 2010). The low value was attributed to the inherent difficulties in floating PGM ores. Bubble load data in conjunction with pulp-phase data and concentrate data were used to describe particle transport across the pulp-froth interface. Two parameters, froth flow number, and net-dropback were introduced. A froth flow number was defined as the ratio of concentrate flow rate to the bubble load flowrate. It was used as a quick way to assess froth performance in the absence of robust entrainment data. A froth flow number greater than one indicates high entrainment if it is known that the bubble load meter is working correctly and a value close to zero indicates high dropback. Net-dropback defined as the difference between bubble load flowrate and concentrate flowrate was also used to understand particle transport dynamics per size class. Where net dropback is positive, particle dropback is dominant and entrainment contribution to concentrate flow is low and when the net-dropback is negative entrainment contribution to the concentrate is high.

The results from this work also indicate that although chromite (regarded as naturally hydrophilic mineral) is thought to be recovered by entrainment, it was also being recovered by true flotation. It was suggested this chromite may be 'locked' in floatable components. This notion was supported by the variation of dropback data which show massive values for fine size classes when compared to larger sizes classes contrary to expectation. It was expected that for the same mineral (chromite) dropback values would be higher for coarser sizes as observed by Rahman et al. (2012). However, in this situation chromite in the coarser size ranges was not rejected by the froth while the fine sizes were hugely rejected. This implies that the larger sizes were not fully liberated and therefore floatable whereas liberated fine chromite is expected to be naturally hydrophilic and easily rejected by the selective froth. The liberation of chromite is expected to increase with a decrease in size class. The susceptibility of liberated chrome particles to detachment and drain back from the froth was high. The data also show high entrainment in the -25µm size class and high dropback of chromite in +25 µm which decreased as

particle sizes increased to -150+106 μm range. The entrained chromite constituted 0.5% of the total concentrate flowrate and is made up of the -25 μm size class.

Acknowledgments

The author would like to thank Lonmin Platinum for allowing experiments to carried out in their concentrator.

References

BHONDAYI, C. 2010. *Measurements of particle loading on bubbles in froth flotation*. MSc dissertation. University of Witwatersrand.

BHONDAYI, C., Moys, M.H., 2011. *Determination of sampling pipe (riser) diameter for aflotation bubble load measuring device*. Minerals Engineering.24, 1664–1676.

CHEGENI, M.H, ABDOLLAHY, M., KHALESI, M.R., 2016. *Bubble loading measurement in a continuous flotation column*. Minerals Engineering. 85, 49–54.

CAWTHORN, R.G. 2005. *Pressure fluctuations and the formation of the PGE-rich Merensky and chromitite reefs*. Bushveld Complex. Mineralium Deposita, 40(2), 231-235.

CAWTHORN, R., 2010. *The Platinum Group Element Deposits of the Bushveld Complex in South Africa*. Platinum Metals Review.

EKMEKCI. Z., BRADSHAW. D.J., ALLISON S.A., HARRIS. P.J., 2003. *Effects of frother type and froth height on the flotation behavior of chromite in UG2 ore*. Minerals Engineering., 16(10), 941–949.

ESKANLOU, A., KHALESI, M.R., ABDOLLAHY, M., 2018. *Interactional effects of bubble size, particle size, and collector dosage on bubble loading in column flotation*. Physicochem. Probl. Miner. Process., 54, 355-362.

DYER, C., 1995. *An investigation into the properties of the froth phase in flotation process*. M.Sc. thesis. University of the Witwatersrand.

HARRIS, T.A., 2000. *Development of a flotation simulation methodology towards an optimisation of UG2 platinum flotation circuits*. PhD thesis. University of Cape Town.

HAY, M.P., ROY, R., 2010, *A case study of optimising UG2 flotation performance, Part 1: Bench, pilot and plant scale factors which influence Cr2O3 entrainment in UG2 flotation*. Mineral Engineering 23 (55–867).

KING, R., HATTON, T., HULBERT, D., 1974. *Bubble loading during flotation*. Transactions of the Institute of Mining and Metallurgy. 83, C112–C115.

MCLAREN, C.H., DE VILLIERS, J.P.R., 1982. *The platinum-group chemistry and mineralogy of the UG-2 chromitite layer of the Bushveld complex*. Economic Geology, 77(6), 1348-1366.

MOYS, M.H., 1978, *A study of a plug flow model for flotation froth behaviour*. Int. J. Miner.Process., 5, 221-238.

MOYS, M.H., 1979. *A study of processes occurring in flotation froths*. PhD thesis. University of Natal.

NEETHLING, S.J., CILLIERS, J.J., 2002. The entrainment of gangue into a flotation froth. Int. J. Miner. Process. 64, 123–134.

PHILLIPS, R.E., JONES, R.T., CHENNELS, P., 2008. *Commercialization of the ConRoast process. Third International Platinum Conference 'Platinum in Transformation'*, The Southern African Institute of Mining and Metallurgy,

RAHMAN. R.M., ATA. S., JAMESON. G.J., 2012. *The effect of flotation variables on the recovery of different particle size fractions in the froth and the pulp*. International Journal of Mineral Processing 106-109, 70 – 77.

SAVASSI, O.N., ALEXANDER, D.J., FRANZIDIS, J-P., MANLAPIG, E.V., 1998. *An empirical model for entrainment in industrial flotation plants*. Miner. Eng. 11, 243–256.

SEAMAN, D. R, FRANZIDIS, J-P., MANLAPIG, E.V., 2004. *Bubble load measurement in the pulp zone of industrial flotation machines – a new device for determining the froth recovery of attached particles*. Int. J. Miner. Process., 74, 1-13.

WESSELDIJK, Q.I., REUTER. M.A., BRADSHAW. D.J., HARRIS, P.J.,1999. *The flotation behaviour of chromite with respect to the beneficiation of UG2 ore*. Miner. Eng., 12, 1177–1184.

YIANATOS, J.B., MOYS, M.H., CONTRERAS, F., VILLANUEVA, A., 2008. *Froth Recovery of industrial flotation cells*. Miner. Eng., 21, 817-827.

YIANATOS, J.B., CONTRERAS. F., 2010. *Particle entrainment model for industrial flotation cells*. Powder Technology 197, 260–267.

ZHENG, X., JOHNSON, N.W., FRANZIDIS, J.P., 2006. *Modelling of entrainment in industrial flotation cells: water recovery and degree of entrainment*. Minerals Engineering., 19, 1191–1203.